Collective mechanisms for atomic transitions in dense plasmas: Representation and screened Coulomb-Born approximation for plasmonic recombination cross sections

F. A. Gutierrez
Departamento de Física, Universidad de Concepción, Casilla 3-C, Concepción, Chile
and Institute for Theoretical Physics, University of California, Santa Barbara, California 93106

M. D. Girardeau
Department of Physics and Institute of Chemical Physics, University of Oregon, Eugene, Oregon 97403
and Institute for Theoretical Physics, University of California, Santa Barbara, California 93106
(Received 26 January 1990)

The Bohm-Pines Fock-Tani representation for a single fixed proton immersed in a finite-temperature electron gas is derived by a sequence of canonical transformations. The long-range correlations between the charged particles of the system give rise to free-bound, bound-free, free-free, and bound-bound hydrogenic transitions with emission or absorption of plasmons by electrons in the field of the fixed proton. These are all exhibited explicitly in the transformed Hamiltonian. Within this "proton in jellium model" differential cross sections for plasmonic recombination into the highly excited and screened levels of hydrogen $(8s,8p,9s,9p)$ for $n_e=10^{18}$ cm^{-3} and $k_BT=0.5$ eV are evaluated using a screened Coulomb (plane-wave) Born approximation. The resulting cross sections appear to be much larger than those expected for the radiative mode.

I. INTRODUCTION

The long-range correlations between the charged particles in plasmas are responsible for the related phenomena of screening and longitudinal plasma oscillations.[1] Screening affects the internal structure of atoms[2] and weakens the strength of atomic transitions significantly near threshold, as shown by explicit calculations performed with screened Debye-Hückel potentials.[3] Plasma oscillations might also play a significant role in the atomic physics of the highest bound levels of the system as suggested by a recently proposed new mechanism for hydrogen recombination in plasmas,[4] whereby the binding energy is carried away by a plasmon (quantum of plasma oscillations) rather than a photon or a third particle. As a generalization of that work, in this paper we shall develop the Bohm-Pines Fock-Tani (BPFT) representation of the Hamiltonian for a simplified model of the plasma, consisting of a single fixed proton immersed in a finite-temperature electron gas. In this transformed Hamiltonian, which exhibits simultaneously all the possible scattering and reaction channels (including the above-mentioned plasmon-mediated recombination mechanism), the particles interact through short-range (screened) potentials while the long-range interactions between them are characterized by emission or absorption of real plasmons. The physical content of the different terms in the expansion of the Hamiltonian will be explained. As an example of application of this representation, we shall evaluate differential cross sections for plasmonic recombination into the highly excited and perturbed levels of hydrogen for plasmas with $n_e=10^{18}$ cm^{-3} and $k_BT=0.5$ eV, using the screened Coulomb (plane-wave) Born approximation. In agreement with semiclassical estimates, the plasmonic recombination cross sections into the perturbed highest levels of hydrogen $(n=8,9)$ are found to be several orders of magnitude larger than those expected for the radiative mode (which are estimated using well-known formulas for the unscreened case). It is pointed out that the plasmonic mode may be comparable to the three-body mode which is usually taken to be the dominant one at these densities.

II. COLLECTIVE REPRESENTATION

Consider a system of volume Ω composed of N_e electrons with density $n_e=N_e/\Omega$, charge e, and mass m_e moving in a uniform immobile positive background whose density is equal to that of the electrons (the electron gas). Working in terms of a Hamiltonian formalism through the use of appropriate canonical transformations, Bohm and Pines[5] obtained a (quantum-mechanical) collective representation of the electron gas as a set of electrons, interacting through short-range screened Coulomb potentials, plus an independent set of plasma oscillations. At temperature T, the Hamiltonian for the electron gas in the collective representation is given, within the random-phase approximation (RPA),[5,6] by[5,7]

$$H^{\mathrm{BP}}=T_e+H_{\mathrm{pl}}+V_{e\text{-}e}+N_e\Delta\ , \tag{1}$$

with

$$\begin{aligned} T_e&=\sum_i P_i^2/2m_e\ ,\\ H_{\mathrm{pl}}&=\sum_{q\,(<q_c)}\hbar\omega_q(C_{\mathbf{q}}^{\dagger}C_{\mathbf{q}}+\tfrac{1}{2})\ ,\\ V_{e\text{-}e}&=\sum_{i,j,k\,(>q_c)}(2\pi e^2/\Omega k^2)e^{i\mathbf{k}\cdot(\mathbf{X}_i-\mathbf{X}_j)}\ ,\\ \Delta&=-\sum_{q\,(<q_c)}(2\pi e^2/\Omega q^2)=-e^2q_c/\pi\ . \end{aligned} \tag{2}$$

Here $\mathbf{P}_i$ is the momentum of the electrons, $C_{\mathbf{q}}$ and $C_{\mathbf{q}}^{\dagger}$ annihilate and create plasmons with momentum $\hbar\mathbf{q}$ and energy $\hbar\omega_q$, q_c is a wave-vector cutoff $\sim\lambda_D^{-1}$, with $\lambda_D=(k_BT/4\pi n_e e^2)^{1/2}$ the Debye screening length for a one-component plasma,[1] and ω_q is the frequency of plasma oscillations defined by the well-known Bohm-Gross dispersion relation[8,9]

$$\omega_q=\omega_p(1+\tfrac{3}{2}\lambda_D^2q^2),\quad q<q_c \tag{3}$$

with $\omega_p=(4\pi n_e e^2/m_e)^{1/2}$. The subsidiary condition on the electronic wave function Ψ,[5]

$$\sum_i\{\omega_q^2/[\omega_q^2-(\mathbf{q}\cdot\mathbf{P}_i/m_e-\hbar q^2/2m_e)^2]\}e^{i\mathbf{q}\cdot\mathbf{X}_i}\Psi=0\ ,\quad q<q_c \tag{4}$$

guarantees that Maxwell's equations are satisfied. In (2), T_e represents the free-electron kinetic energy, $H_{\rm pl}$ the free plasmons, $V_{e\text{-}e}$ a screened electron-electron interaction,[10] and Δ a constant negative-energy shift that results from the long-range correlations between the electrons.[11] The independence of the collective behavior (plasmons) from the single-particle motion is certainly an approximation, because at nonzero temperature there is always at least a slight probability of finding an electron of wave vector $\mathbf{k}$ such that it is capable of absorbing a plasmon of wave vector $\mathbf{q}$ with conservation of momentum and energy, producing a damping of the oscillations. This linear Landau damping[12] is contained in the imaginary component of the complex frequency $\Omega_q=\omega_q-i\gamma_q$. For a Maxwellian electron distribution,[12]

$$\gamma_q/\omega_p\approx\pi^{1/2}[\omega_q/q(2k_BT/m_e)^{1/2}]^3e^{-1/2(q\lambda_D)^2}\ . \tag{5}$$

Therefore, for those q such that $q\lambda_D\ll1$, the damping is negligible, and we can (in a good approximation) consider the plasmon modes as independent degrees of freedom of the system. An equivalent argument uses the fact that a charged particle traveling through the plasma with velocity $\mathbf{v}$ can emit a real plasmon of momentum $\hbar\mathbf{q}$ and energy $\hbar\omega_q$, with conservation of momentum and energy, only if the condition $\omega_q=\mathbf{q}\cdot\mathbf{v}$ is satisfied.[1,6] Since there is a maximum plasmon wave vector q_c, there is a critical velocity $v_c\sim\omega_p\lambda_D$ below which real plasmon emission cannot occur. Thus, for the finite-temperature electron gas, only the few electrons in the high-velocity tail of the Maxwellian distribution will have enough velocity to excite plasmons. For this reason Bohm and Gross (BG) neglected this contribution to obtain the dispersion relation (3). In doing this they neglected a small coupling between electrons and plasmons analogous to what we do here in the context of Bohm-Pines (BP) theory.

Consider now a single proton of charge e immersed in the electron gas and fixed at the origin. Its interaction with the electron gas is given by the expression

$$-\sum_{i,K}(4\pi e^2/\Omega K^2)e^{i\mathbf{K}\cdot\mathbf{X}_i}\ , \tag{6}$$

which under BP transformation[13] gets transformed into[14]

$$\begin{aligned}
&-\sum_{\substack{i,K\\K\,(>q_c)}}(4\pi e^2/\Omega K^2)e^{i\mathbf{K}\cdot\mathbf{X}_i}-\sum_{\substack{i,K\\K\,(<q_c)}}(4\pi e^2/\Omega K^2)e^{i\mathbf{K}\cdot\mathbf{X}_i}\\
&-\left[\sum_{\substack{i,K,q\\q\,(<q_c)\\K\,(>q_c)}}(4\pi e^2/\Omega K^2)(2\pi e^2\omega_q/\Omega\hbar q^2)^{1/2}e^{i(\mathbf{K}-\mathbf{q})\cdot\mathbf{X}_i}g(\mathbf{q},\mathbf{P}_i,-\mathbf{K})\hat{C}_{\mathbf{q}}^{\dagger}+\text{H.c.}\right]\\
&-\left[\sum_{\substack{i,K,q\\q\,(<q_c)\\K\,(<q_c)}}(4\pi e^2/\Omega K^2)(2\pi e^2\omega_q/\Omega\hbar q^2)^{1/2}e^{i(\mathbf{K}-\mathbf{q})\cdot\mathbf{X}_i}g(\mathbf{q},\mathbf{P}_i,-\mathbf{K})\hat{C}_{\mathbf{q}}^{\dagger}+\text{H.c.}\right]\\
&-\sum_{q\,(<q_c)}(2\pi e^2\hbar\omega_q/\Omega q^2)^{1/2}(\hat{C}_{\mathbf{q}}^{\dagger}+\hat{C}_{\mathbf{q}})+\cdots\ ,
\end{aligned} \tag{7}$$

where the ellipsis represents higher order terms, and

$$g(\mathbf{q},\mathbf{P}_i,\mathbf{K})=\left[\omega_q-\frac{\mathbf{q}\cdot\mathbf{P}_i}{m_e}+\frac{\hbar q^2}{2m_e}+\frac{\hbar\mathbf{q}\cdot\mathbf{K}}{m_e}\right]^{-1}-\left[\omega_q-\frac{\mathbf{q}\cdot\mathbf{P}_i}{m_e}+\frac{\hbar q^2}{2m_e}\right]^{-1}\ . \tag{8}$$

In (7), H.c. stands for Hermitian conjugate, and, since the "higher-order terms" are of the same order of magnitude as those neglected in deriving the Hamiltonian (1), we do not consider them any further. The first term in (7) represents a screened electron-proton interaction which has the same form as the electron-electron interaction $V_{e\text{-}e}$ appearing in (2).[10,15] Applying the subsidiary condition (4) to the second term in (7) yields

$$\sum_{\substack{i,K\\K\,(<q_c)}}\left[\frac{4\pi e^2}{\Omega K^2}\right]\frac{(\mathbf{K}\cdot\mathbf{P}_i/m_e-\hbar K^2/2m_e)^2}{[\omega_K^2-(\mathbf{K}\cdot\mathbf{P}_i/m_e-\hbar K^2/2m_e)^2]}e^{i\mathbf{K}\cdot\mathbf{X}_i}\ . \tag{9}$$

By our taking the thermal average of (9) and using the assumption of isotropy of the K's, it is found[10,15] that (9) tends to cancel the small oscillations contained in the first term in (7) that occur for distances larger than λ_D. Since we are neglecting these oscillations in the present work,[10,15] then it is consistent to neglect the contributions coming from the second term in (7). Similarly, the fourth term in (7) may be neglected when compared with the third term; first, because the values of $g(\mathbf{q},\mathbf{P}_i,-\mathbf{K})$ in the region $K<q_c$ are very small compared with the values of the same function in the region $K>q_c$ (as can be easily verified); and second, because the subsidiary condition (4) reduces the fourth term by a factor $\sim(\mathbf{K}\cdot\mathbf{P}_i/m_e\omega_K)^2\ll 1$ for $K<q_c$. The last term in (7) represents the absorption and emission of virtual plasmons by the fixed proton leading, as shown in Ref. 4 [Eq. (6)], to a negative shift (Δ) of the energy. Therefore, the total Hamiltonian for the electron gas plus the fixed proton, in BP representation further transformed into Fock space, is

$$\hat{H}_{p+\mathrm{pl}}=\hat{T}_e+\hat{H}_{\mathrm{pl}}+\hat{V}_{e\text{-}e}+\hat{V}_{e\text{-}p}+\hat{V}_{e\text{-pl}}+(N_e+1)\Delta\ , \tag{10}$$

with

$$\begin{aligned}
\hat{T}_e&=\sum_{k}(\hbar^2k^2/2m_e)\hat{e}^{\dagger}_{\mathbf{k}}\hat{e}_{\mathbf{k}}\ ,\\
\hat{H}_{\mathrm{pl}}&=\sum_{q\,(<q_c)}\hbar\omega_q(\hat{C}^{\dagger}_{\mathbf{q}}C_{\mathbf{q}}+\tfrac{1}{2})\ ,\\
\hat{V}_{e\text{-}e}&=\sum_{\substack{k,k',K\\K\,(>q_c)}}(2\pi e^2/\Omega K^2)\hat{e}^{\dagger}_{\mathbf{k}+\mathbf{K}}\hat{e}^{\dagger}_{\mathbf{k}'-\mathbf{K}}\hat{e}_{\mathbf{k}'}\hat{e}_{\mathbf{k}}\ ,\\
\hat{V}_{e\text{-}p}&=-\sum_{\substack{k,K\\K\,(>q_c)}}(4\pi e^2/\Omega K^2)\hat{e}^{\dagger}_{\mathbf{k}+\mathbf{K}}\hat{e}_{\mathbf{k}}\ ,\\
\hat{V}_{e\text{-pl}}&=\sum_{\substack{k,K,q\\K\,(>q_c)\\q\,(<q_c)}}(4\pi e^2/\Omega K^2)(2\pi e^2\omega_q/\Omega\hbar q^2)^{1/2}\\
&\qquad\times\xi_{\mathbf{qkK}}(\hat{C}^{\dagger}_{\mathbf{q}}\hat{e}^{\dagger}_{\mathbf{k}-\mathbf{q}+\mathbf{K}}\hat{e}_{\mathbf{k}}+\mathrm{H.c.})\ .
\end{aligned} \tag{11}$$

Here $\hat{e}_{\mathbf{k}}$ and $\hat{e}^{\dagger}_{\mathbf{k}}$ annihilate and create electrons with momentum $\hbar\mathbf{k}$ and

$$\xi_{\mathbf{qkK}}=(\omega_q-\hbar\mathbf{q}\cdot\mathbf{k}/m_e)^{-1}-[\omega_q-(\hbar/m_e)\mathbf{q}\cdot(\mathbf{k}+\mathbf{K})]^{-1}\ , \tag{12}$$

where we have neglected terms of order q^2 for $q<q_c$; these represent pure quantum effects and are very small (less than 1% of ω_q for $n_e\sim 10^{18}$ cm^{-3} and $k_BT\sim 1$ eV). The Hamiltonian (10) has been already quoted without any derivation in Ref. 4 [see Eqs. (2), (6), and (7), and related comments]. Several remarks concerning the different terms in this Hamiltonian can be found there. Here we only want to emphasize the fact that the presence of the extra proton is crucial for the existence of the term $V_{e\text{-pl}}$, the electron-plasmon interaction with emission and absorption of single plasmons by electrons in the field of the proton. Indeed, it is the proton-electron attraction which allows the incoming electron to increase its velocity until it exceeds the critical velocity v_c mentioned before to emit a real plasmon. This interpretation of the emission process is contained in the singularities of ξ:

$$\omega_q=\begin{cases}\mathbf{q}\cdot\mathbf{v}_k, & q<q_c \qquad (13)\\ \mathbf{q}\cdot[\mathbf{v}_k+\hbar\mathbf{K}/m_e], & q<q_c \qquad (14)\end{cases}$$

where $\mathbf{v}_k\equiv\hbar\mathbf{k}/m_e$ is interpreted as the random (classical) velocity of the electrons in the plasma, and $\hbar\mathbf{K}/m_e$ represents the increase in velocity of the electrons produced by the short-range ($K>q_c$) attractive interaction with the proton. The first singularity is the previously mentioned condition for real-plasmon emission which, for the electron gas, will be satisfied only by the few electrons in the high-velocity tail of the Maxwellian distribution; therefore, we neglect it. On the contrary, the second singularity cannot be neglected because the sum on K appearing in $V_{e\text{-pl}}$ ensures that for any $\mathbf{v}_k$ there is always a $\mathbf{K}$ such that the condition (14) is satisfied. Thus even a slow electron in the field of the proton can increase its velocity to emit a real plasmon.

III. BPFT HAMILTONIAN

Another change of representation is useful to separate explicitly the free-electron states from the bound-electron states. In fact, in the new representation, all the different reaction channels of the system will be displayed explicitly as separate terms in the Hamiltonian. The required canonical transformation, which is a particular case (fixed proton) of the general Fock-Tani transformation,[16] is effected by a unitary operator $\hat{U}$ given by[17]

$$\hat{U}=e^{(\pi/2)\hat{F}},\quad \hat{F}=\sum_{\nu}(\hat{A}^{\dagger}_{\nu}\hat{a}_{\nu}-\hat{a}^{\dagger}_{\nu}\hat{A}_{\nu})\ , \tag{15}$$

where $\hat{A}_{\nu}$ and $\hat{A}^{\dagger}_{\nu}$ are the (Fermi) annihilation and creation operators for electrons bound in (here perturbed) hydrogen orbitals centered on the proton at the origin:

$$\hat{A}^{\dagger}_{\nu}=\sum_{k}\tilde{\phi}_{\nu}(\mathbf{k})\hat{e}^{\dagger}_{\mathbf{k}},\quad \hat{A}_{\nu}=(\hat{A}^{\dagger}_{\nu})^{\dagger}\ . \tag{16}$$

The index ν stands for (n,l,m) (and the spin z component s, which will be suppressed here); $\tilde{\phi}_{\nu}(\mathbf{k})$ is the (perturbed) hydrogen momentum wave function, the Fourier transform of the perturbed spatial wave function $\phi_{\nu}(\mathbf{x})$. The new bound-state Fermi annihilation and creation operators $\hat{a}_{\nu}$ and $\hat{a}^{\dagger}_{\nu}$ introduced by this transformation anticommute with the original (plane-wave) electron operators $\hat{e}_{\mathbf{k}}$ and $\hat{e}^{\dagger}_{\mathbf{k}}$ (although the $\hat{e}_{\mathbf{k}}$ and $\hat{A}^{\dagger}_{\nu}$ do not anticommute) and they commute with the plasmon operators $\hat{C}_{\mathbf{q}}$ and $\hat{C}^{\dagger}_{\mathbf{q}}$. The canonical transformation effected by (15) is

$$\hat{U}^{-1}\hat{e}_{\mathbf{k}}\hat{U}=\hat{e}_{\mathbf{k}}-\sum_{k'}\Delta_{\mathbf{k},\mathbf{k}'}\hat{e}_{\mathbf{k}'}+\sum_{\nu}\tilde{\phi}_{\nu}(\mathbf{k})\hat{a}_{\nu}\ , \tag{17}$$

where $\Delta_{\mathbf{k},\mathbf{k}'}$ is the bound-state kernel

$$\Delta_{\mathbf{k},\mathbf{k}'}=\sum_{\nu}\tilde{\phi}_{\nu}(\mathbf{k})\tilde{\phi}^{*}_{\nu}(\mathbf{k}')\ . \tag{18}$$

Insertion of (17) into (12) yields after some lengthy alge-

bra the Bohm-Pines Fock-Tani representation of the Hamiltonian for a fixed proton immersed in an electron gas. It has the structure[18]

$$H=(N_e+1)\Delta+H_{\rm pl}+T_e+H_a+H_{p\text{-}e}+H(a\leftarrow e)+H(e\leftarrow a)+H({\rm pl}\,a\leftarrow e)+H(e\leftarrow{\rm pl}\,a)+H(e\leftarrow{\rm pl}\,e)+H({\rm pl}\,a\leftarrow a)+H(a\leftarrow{\rm pl}\,a)+V_{e\text{-}e}+H(ea\leftarrow ee)+H(ee\leftarrow ea)+H_{ae}+\cdots \quad (19)$$

In (19), Δ, $H_{\rm pl}$, and T_e are the same terms as those before the transformation (17), except that the physical interpretation of T_e is different now in that the $\hat{e}_{\mathbf{k}}$ and $\hat{e}^{\dagger}_{\mathbf{k}}$ operators refer only to unbound electrons. The diagrammatic representation of T_e is shown in Fig. 1. Incoming lines approach from the right and stand for annihilation operators on the right in the corresponding term in the Hamiltonian; outgoing lines leave toward the left and stand for creation operators on the left in the same term.[18]

H_a is a screened single-atom Hamiltonian, $H(e\leftarrow a)$ and $H(a\leftarrow e)$ the Hamiltonians for ionization and recombination processes, and $H_{p\text{-}e}$ an effective interaction between the proton and the free electrons modified by the presence of bound-electron states:

$$\begin{aligned} H_a&=\sum_{\mu,\nu}\hat{a}^{\dagger}_{\mu}(\mu|V_a|\nu)\hat{a}_{\nu}\ ,\\ H(e\leftarrow a)&=\sum_{k,\nu}\hat{e}^{\dagger}_{\mathbf{k}}(k|V(e\leftarrow a)|\nu)\hat{a}_{\nu}\ ,\\ H(a\leftarrow e)&=[H(a\leftarrow e)]^{\dagger}\ ,\\ H_{p\text{-}e}&=\sum_{k',k}\hat{e}^{\dagger}_{\mathbf{k}'}(k'|V_{p\text{-}e}|k)\hat{e}_{\mathbf{k}}\ , \end{aligned} \quad (20)$$

where

$$\begin{aligned} (\mu|V_a|\nu)&=\int\phi^{*}_{\nu}(\mathbf{x})H(\mathbf{x})\phi_{\mu}(\mathbf{x})d^3x\ ,\\ (k|V(e\leftarrow a)|\nu)&=F_{\nu}(\mathbf{k})-\sum_{k'}F_{\nu}(\mathbf{k}')\Delta_{\mathbf{k},\mathbf{k}'}\ , \end{aligned} \quad (21)$$

$$(k'|V_{p\text{-}e}|k)=\sum_{K\,(>q_c)}(-4\pi e^2/\Omega K^2)\delta_{\mathbf{k}',\mathbf{k}+\mathbf{K}}-\sum_{\nu}F_{\nu}(\mathbf{k}')\tilde{\phi}^{*}_{\nu}(\mathbf{k})-\sum_{\nu}F^{*}_{\nu}(\mathbf{k})\tilde{\phi}_{\nu}(\mathbf{k}')+\sum_{k''}\Delta_{\mathbf{k}'',\mathbf{k}}\sum_{\nu}F_{\nu}(\mathbf{k}'')\tilde{\phi}_{\nu}(\mathbf{k}')\ ,$$

with

$$H(\mathbf{x})=\frac{-\hbar^2\nabla^2}{2m_e}+\sum_{K\,(>q_c)}(-4\pi e^2/\Omega K^2)e^{i\mathbf{K}\cdot\mathbf{x}} \quad (22)$$

the Hamiltonian of a single electron in the screened Coulomb field of the proton, and

$$F_{\nu}(\mathbf{k})=\frac{\hbar^2k^2}{2m_e}\tilde{\phi}_{\nu}(\mathbf{k})+\sum_{K\,(>q_c)}(-4\pi e^2/\Omega K^2)\tilde{\phi}_{\nu}(\mathbf{k}+\mathbf{K})\ . \quad (23)$$

The diagrams corresponding to these transitions are given in Fig. 2. The dashed lines stand for the fixed proton and the double lines for the electrons bound to it. Interaction Hamiltonians analogous to (20) have been obtained previously by Girardeau[16] for a more general system consisting of many electrons, protons, and atoms (e.g., a partially ionized atomic hydrogen plasma). However, in that work there was no attempt to study the long-range correlations between the particles, so that screening and plasma oscillations did not appear, these effects being concealed in the long range of the Coulomb force between the "bare particles" of the system. Screening for the electron-proton pair in our case is a consequence of the fact that we are not only considering the "bare electron-proton pair" but also the contributions (within the RPA) coming from all the electrons that compose the rest of the system. This RPA is approximately equivalent to the sum of the ring diagrams for the finite-temperature electron gas in many-body theory,[19] which is the sum of an infinite series of divergent terms (because of the infinite range of the Coulomb force) that give rise to screening. Therefore, our formulas are more suitable to direct application than those in the above-mentioned work, especially for high-density plasmas where the medium strongly perturbs the reactions. If the ϕ_{ν}'s are chosen to be energy eigenstates of the screened Hamiltonian $H(\mathbf{x})$ with energy ε_{ν}, then with (22) and (23) we have

$$H(\mathbf{x})\phi_{\nu}(\mathbf{x})=\varepsilon_{\nu}\phi_{\nu}(\mathbf{x}),\quad F_{\nu}(\mathbf{k})=\varepsilon_{\nu}\tilde{\phi}_{\nu}(\mathbf{k})\ , \quad (24)$$

where $\tilde{\phi}_{\nu}(\mathbf{k})$ is the Fourier transform of the energy eigen-

FIG. 1. Diagram representing the electron kinetic energy T_e.

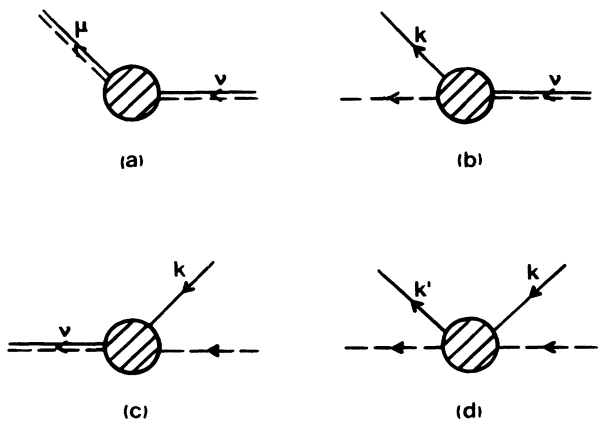

FIG. 2. Diagrams for (a) single-atom Hamiltonian H_a, (b) $H(e\leftarrow a)$, (c) $H(a\leftarrow e)$, and (d) $H_{p\text{-}e}$. Dashed lines stand for the fixed proton and double lines for hydrogen atoms.

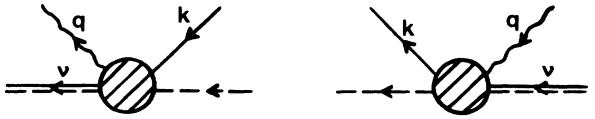

FIG. 3. Representation of plasmonic-recombination and plasmonic-ionization Hamiltonians. Wavy lines represent plasmons.

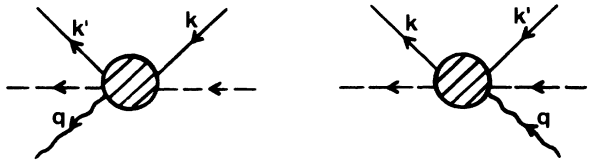

FIG. 4. Diagrams for free-free electron transitions in the field of the proton by plasmon emission and plasmon absorption.

state $\phi_\nu(\mathbf{x})$. Thus (21) gets reduced to

$$\begin{aligned}
&(\mu|V_a|\nu)=\varepsilon_\nu\delta_{\mu\nu}\ ,\\
&(k|V(e\leftarrow a)|\nu)=0\ ,\\
&(k'|V_{p\text{-}e}|k)=\sum_{K\,(>q_c)}(-4\pi e^2/\Omega K^2)\delta_{\mathbf{k}',\mathbf{k}+\mathbf{K}}\\
&\qquad\qquad-\sum_\nu \varepsilon_\nu\tilde{\phi}_\nu(\mathbf{k}')\tilde{\phi}^*_\nu(\mathbf{k})\ ,
\end{aligned}\tag{25}$$

where the orthonormality of the bound states $\phi_\nu(\mathbf{x})$ [or $\tilde{\phi}_\nu(\mathbf{k})$] has been used. The first equation in (25) tells us that the state ν propagates without decaying into other atomic states μ. If there were external fields, then the ϕ's satisfying (24) would not be eigenstates of the total Hamiltonian (external field included), and the nondiagonal matrix elements would not vanish. The second equality is again a consequence (together with the first equality) of the stability of the single-atom screened energy eigenstates in the absence of external perturbations, so that the breaking of the atom into its components does not occur in these circumstances. In the last equality, the first term at the right is the screened Coulomb interaction between the proton and the electrons, whereas the second term is the portion of the spectral representation of the Hamiltonian $H(\mathbf{x})$ associated with all of its bound states. Therefore, $(k'|V_{p\text{-}e}|k)$ should not have any bound state, while it should be equivalent to the screened Coulomb potential when acting on a continuum (unbound) energy eigenstate.

The next six terms in the Hamiltonian (19), which contain a plasmon operator in the initial or in the final state, arise as a consequence of applying the canonical transformation (17) to $\hat{V}_{e\text{-pl}}$ in (12). The interaction terms $H(\mathrm{pl}\,a\leftarrow e)$ and $H(e\leftarrow\mathrm{pl}\,a)$ given by

$$\begin{aligned}
&H(\mathrm{pl}\,a\leftarrow e)=\sum_{\substack{k,q,\nu\\ q\,(<q_c)}}\hat{a}^\dagger_\nu\hat{C}^\dagger_{\mathbf{q}}(\nu q|V(\mathrm{pl}\,a\leftarrow e)|k)\hat{e}_{\mathbf{k}}\ ,\\
&H(e\leftarrow\mathrm{pl}\,a)=[H(\mathrm{pl}\,a\leftarrow e)]^\dagger\ ,
\end{aligned}\tag{26}$$

with

$$\begin{aligned}
&(\nu q|V(\mathrm{pl}\,a\leftarrow e)|k)\\
&\quad=\sum_{K\,(>q_c)}(4\pi e^2/\Omega K^2)(2\pi e^2\omega_q/\Omega\hbar q^2)^{1/2}\\
&\qquad\times\left[\xi_{\mathbf{q},\mathbf{k},\mathbf{K}}\tilde{\phi}^*_\nu(\mathbf{k}-\mathbf{q}+\mathbf{K})\right.\\
&\qquad\left.-\sum_{k'}\Delta_{\mathbf{k}',\mathbf{k}}\xi_{\mathbf{q},\mathbf{k}',\mathbf{K}}\tilde{\phi}^*_\nu(\mathbf{k}'-\mathbf{q}+\mathbf{K})\right]\ ,
\end{aligned}\tag{27}$$

and with diagrammatic representations displayed in Fig. 3, are responsible for the mechanism of plasmonic recombination (to highly excited states of hydrogen) and for the inverse ionization process, as reported in Ref. 4. In (27) the sum on K together with the function $\xi_{\mathbf{q},\mathbf{k},\mathbf{K}}$ characterize the plasmon emission while the momentum wave functions $\tilde{\phi}_\nu(\mathbf{k})$ characterize the final bound electron. In lowest-order approximation, the wave functions $\tilde{\phi}_\nu(\mathbf{k})$ can be taken to be eigenstates of the screened Coulomb potential, satisfying Eq. (24). As already mentioned in Ref. 4, with this choice one neglects the imaginary part of the atomic self-energy, i.e., the finite lifetime of the perturbed atomic state. The subtraction term involving the bound-state kernel $\Delta_{\mathbf{k},\mathbf{k}'}$ orthogonalizes the k dependence of the matrix element to the bound electron subspace to take into account the fact that $\hat{e}_{\mathbf{k}}$ annihilates an initially unbound electron. The Hamiltonian $H(\mathrm{pl}\,e\leftarrow e)$ describes free-free electron transitions in the field of the fixed proton with plasmon emission, and $H(e\leftarrow\mathrm{pl}\,e)$ the corresponding transition with absorption of a plasmon. The diagrams for these processes are shown in Fig. 4, and the explicit expressions are

$$\begin{aligned}
&H(\mathrm{pl}\,e\leftarrow e)=\sum_{\substack{k,k',q\\ q\,(<q_c)}}\hat{e}^\dagger_{\mathbf{k}'}\hat{C}^\dagger_{\mathbf{q}}(k'q|V(\mathrm{pl}\,e\leftarrow e)|k)\hat{e}_{\mathbf{k}}\ ,\\
&H(e\leftarrow\mathrm{pl}\,e)=[H(\mathrm{pl}\,e\leftarrow e)]^\dagger\ ,
\end{aligned}\tag{28}$$

with

$$\begin{aligned}
(k'q|V(\mathrm{pl}\,e\leftarrow e)|k)&=\sum_{K\,(>q_c)}(4\pi e^2/\Omega K^2)(2\pi e^2\omega_q/\Omega\hbar q^2)^{1/2}\\
&\times\left[\xi_{\mathbf{q},\mathbf{k},\mathbf{K}}[\delta_{\mathbf{k}',\mathbf{k}+\mathbf{K}+\mathbf{q}}-(\Delta_{\mathbf{k}',\mathbf{k}+\mathbf{K}-\mathbf{q}}+\Delta_{\mathbf{k},\mathbf{k}'-\mathbf{K}+\mathbf{q}})]+\sum_{k''}\xi_{\mathbf{q},\mathbf{k}'',\mathbf{K}}\Delta_{\mathbf{k}',\mathbf{k}''+\mathbf{K}-\mathbf{q}}\Delta_{\mathbf{k}'',\mathbf{k}}\right]\ .
\end{aligned}\tag{29}$$

It should be emphasized that this mode of (plasmon) emission is different than the one induced by the few electrons in the high-velocity tail of the Maxwellian distribution (related to Landau damping) and which we have neglected within the BG approximation. Indeed, in (29) even very slow electrons in the attractive field of the proton can start to speed up until they reach the critical velocity for plasmon emission. The presence of bound electrons modifies the matrix elements for free-free electron transitions of the proton because of the fact that the free electrons have wave functions orthogonal to the bound states. These modifications are represented by the last three (orthogonalization) terms in (29). Other atomic processes are bound-bound transitions with emission and absorption of plasmons represented by $H(\mathrm{pl}\,a\leftarrow a)$ and $H(a\leftarrow\mathrm{pl}\,a)$, respectively:

$$H(\mathrm{pl}\,a\leftarrow a)=\sum_{\substack{q,\nu,\mu\\ q\,(<q_c)}}\hat{a}_\nu^\dagger\hat{C}_{\mathbf{q}}^\dagger(\nu q|V(\mathrm{pl}\,a\leftarrow a)|\mu)\hat{a}_\mu\ ,$$

$$H(a\leftarrow\mathrm{pl}\,a)=[H(\mathrm{pl}\,a\leftarrow a)]^\dagger\ , \tag{30}$$

with

$$(\nu q|V(\mathrm{pl}\,a\leftarrow a)|\mu)$$

$$=\sum_{\substack{k,K\\ K\,(>q_c)}}(4\pi e^2/\Omega K^2)(2\pi e^2\omega_q/\Omega\hbar q^2)^{1/2}$$

$$\times\xi_{\mathbf{q},\mathbf{k},\mathbf{K}}\tilde{\phi}_\nu^*(\mathbf{k}-\mathbf{q}+\mathbf{K})\tilde{\phi}_\mu(\mathbf{k})\ , \tag{31}$$

and with diagrams shown in Fig. 5. As in the case of free-bound and free-free transitions induced by the plasmon field, the matrix elements (31) contain the function $\xi_{\mathbf{q},\mathbf{k},\mathbf{K}}$, whose singularities have been interpreted as a manifestation of the collective excitation of a plasmon, represented in this case by the operator $\hat{C}_{\mathbf{q}}^\dagger$ in (30). The last two terms in the Hamiltonian (19) containing plasmon operators are described by $H(\mathrm{pl}\,e\leftarrow a)$ and $H(a\leftarrow\mathrm{pl}\,e)$, where

$$H(\mathrm{pl}\,e\leftarrow a)=\sum_{\substack{k,q,\nu\\ q\,(<q_c)}}\hat{e}_{\mathbf{k}}^\dagger\hat{C}_{\mathbf{q}}^\dagger(kq|V(\mathrm{pl}\,e\leftarrow a)|\nu)\hat{a}_\nu\ ,$$

$$H(a\leftarrow\mathrm{pl}\,e)=[H(\mathrm{pl}\,e\leftarrow a)]^\dagger\ , \tag{32}$$

with

$$(kq|V(\mathrm{pl}\,e\leftarrow a)|\nu)$$

$$=\sum_{K\,(>q_c)}(4\pi e^2/\Omega K^2)(2\pi e^2\omega_q/\Omega\hbar q^2)^{1/2}$$

$$\times\left[\xi_{\mathbf{q},\mathbf{k}+\mathbf{q}-\mathbf{K},\mathbf{K}}\tilde{\phi}_\nu(\mathbf{k})-\sum_{k'}\Delta_{\mathbf{k},\mathbf{k}'}\xi_{\mathbf{q},\mathbf{k}'+\mathbf{q}-\mathbf{K},\mathbf{K}}\tilde{\phi}_\nu(\mathbf{k}')\right]\ . \tag{33}$$

Relations (32) represent spontaneous breaking of the atom into a plasmon and a free electron (plus the fixed proton), and the inverse process of plasmon-induced recombination, whose diagrams appear in Fig. 6. Within the BG approximation and considering the single-atom energy eigenstates (24), we have that the terms with large parentheses in the matrix elements (33) reduce to

$$\xi_{\mathbf{q},-\mathbf{K},\mathbf{K}}\left[\tilde{\phi}_\nu(\mathbf{k})-\sum_{k'}\tilde{\phi}_\nu(\mathbf{k}')\Delta_{\mathbf{k},\mathbf{k}'}\right]=0 \tag{34}$$

in a way analogous to the second equation in (25). Again, the situation is that in the absence of external perturbations, the atom is stable so that the matrix elements (33) vanish.

The other terms in the Hamiltonian (19) arise as a consequence of applying (17) to the short-range (screened Coulomb) electron-electron interaction $V_{e\text{-}e}$. Their expli-

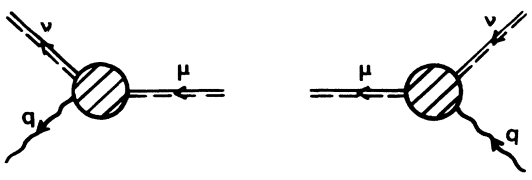

FIG. 5. Diagrammatic representation of bound-bound transitions of the atom induced by emission and absorption of plasmons.

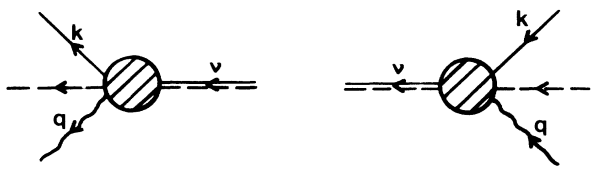

FIG. 6. Diagrammatic representation of $H(\mathrm{pl}\,e\leftarrow a)$ and $H(a\leftarrow\mathrm{pl}\,e)$.

cit expressions are

$$V_{e\text{-}e}=\sum_{\substack{k,k',K\\K\,(>q_c)}}(2\pi e^2/\Omega K^2)\hat{e}^{\dagger}_{\mathbf{k}+\mathbf{K}}\hat{e}^{\dagger}_{\mathbf{k}'-\mathbf{K}}\hat{e}_{\mathbf{k}'}\hat{e}_{\mathbf{k}}\ ,$$

$$H(ee\leftarrow ea)=\sum_{\substack{k,k',K,\nu\\K\,(>q_c)}}(4\pi e^2/\Omega K^2)\tilde{\phi}_{\nu}(\mathbf{k})\hat{e}^{\dagger}_{\mathbf{k}+\mathbf{K}}\hat{e}^{\dagger}_{\mathbf{k}'-\mathbf{K}}\hat{e}_{\mathbf{k}'}\hat{a}_{\nu}\ , \tag{35}$$

$$H(ea\leftarrow ee)=[H(ee\leftarrow ea)]^{\dagger}\ ,$$

$$H(ea\leftarrow ea)=-\sum_{\substack{k,k',\mu,\nu,K\\K\,(>q_c)}}(4\pi e^2/\Omega K^2)\tilde{\phi}^{*}_{\nu}(\mathbf{k}'-\mathbf{K})\tilde{\phi}_{\mu}(\mathbf{k}')\times(\hat{e}^{\dagger}_{\mathbf{k}+\mathbf{K}}\hat{a}^{\dagger}_{\nu}\hat{a}_{\mu}\hat{e}_{\mathbf{k}}-\hat{e}^{\dagger}_{\mathbf{k}'+\mathbf{K}}\hat{a}^{\dagger}_{\nu}\hat{a}_{\mu}\hat{e}_{\mathbf{k}})\ ,$$

with

$$\hat{e}_{\mathbf{k}}\equiv\hat{e}_{\mathbf{k}}-\sum_{k'}\Delta_{\mathbf{k},\mathbf{k}'}\hat{e}_{\mathbf{k}'},\quad \hat{e}^{\dagger}_{\mathbf{k}}=(\hat{e}_{\mathbf{k}})^{\dagger}\ , \tag{36}$$

and with diagrams given in Fig. 7. We have expressed the interaction Hamiltonians (35) in terms of the orthogonalized plane-wave operators $\hat{e}_{\mathbf{k}}$ and $\hat{e}^{\dagger}_{\mathbf{k}}$ (Ref. 20) to keep the expressions compact, although it is straightforward to express them in terms of the free plane-wave operators $\hat{e}_{\mathbf{k}}$ and $\hat{e}^{\dagger}_{\mathbf{k}}$ by use of relation (36). The term $V_{e\text{-}e}$ gives the short-range ($K>q_c$) electron-electron collisions in the field of the proton. The effect of the bound states on this reaction is apparent from the fact that the electrons are described by plane waves orthogonalized to the bound states, the electrons being free before and after the interaction with no possible binding to the proton. The binding of one of the electrons after the interaction is described by $H(ea\leftarrow ee)$, which represents the process of three-body (two electrons plus the fixed proton) hydrogen recombination. The inverse process of collisional ionization is described by $H(ee\leftarrow ea)$. Finally, electron-atom scattering and the electron exchange between a free electron and the bound electron are given as the first and second terms of $H(ea\leftarrow ea)$ in (35). As was the case with some other terms in the Hamiltonian (19) [see Eqs. (20)–(23) and related comments], there exists unscreened analogs of the interaction Hamiltonians (35). As mentioned before, here we take into account, through BP theory,[5] the effects of the medium on the reactions. One of these effects is the (static) screening of the field of the particles which shorten the range of effective interactions to distances of the order of λ_D. This fact is made explicit by the constraint $K>q_c$ in the sum of K in (35), with $q_c\sim\lambda_D^{-1}$. Although dynamical screening of tightly bound states is very small and overestimated by static (Debye) screening, we are concerned in this paper primarily with loosely bound states for which static screening is a good first approximation.

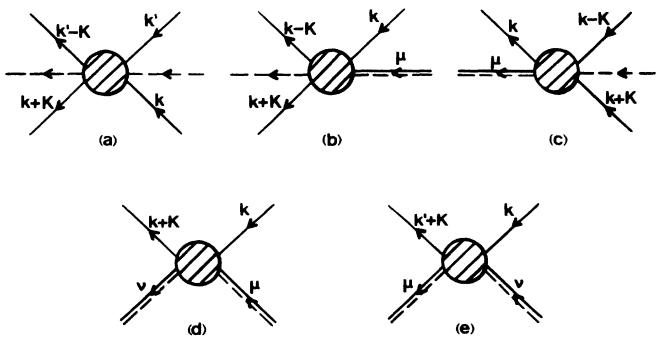

FIG. 7. Representation for (a) short-range electron-electron collisions in the field of the proton, (b) collisional ionization, (c) three-body hydrogen recombination, (d) electron-atom scattering, and (e) electron-exchange reaction.

All the contributions to (19) have been described. The omitted terms (within the RPA) are those containing more than one bound electron in the initial and/or final state. As an example of the application of the representation, we calculate in Sec. IV the plasmonic recombination cross sections (in Born approximation) to the highly excited and perturbed levels of hydrogen. Explicit evaluations are made for $n_e=10^{18}$ cm^{-3}, $k_BT=0.5$ eV, and $(q\lambda_D)^2=0.1$. This mechanism was recently proposed,[4] and more recently an evaluation of the transition rates for Al at metallic densities was carried out.[21] Plasmonic recombination is energetically allowed because the plasmon energies are larger or of the same order of magnitude as the binding energies of the highly excited and perturbed states of hydrogen. In a similar way it is found that plasmon energies also match energy differences between highly excited states of hydrogen, so that bound-bound transitions induced by the collective field are also energetically allowed. Examples of this situation are the transitions $8s\rightarrow 7g$ and $8p\rightarrow 7f$ (Ref. 22) for $k_BT\sim 0.5$ eV, $n_e\sim 10^{18}$ cm^{-3}, and $(q\lambda_D)^2\sim 0.1$. For free-free emission, and because of the continuum of energies for the initial and final states, the only requirement for the process to occur is that the electron in the field of the proton be able to reach the critical velocity v_c for real-plasmon emission. In semiclassical terms this requirement is met by incoming electrons with a sufficiently small impact parameter (see Appendix A).

IV. PLASMON-MEDIATED RECOMBINATION

A rough estimate of the order of magnitude of the plasmonic recombination cross section can be obtained with the help of the expression

$$\sigma_{\rm sc}\approx 17[(\hbar\omega_p)^{3/2}/(k_BT)^{9/2}]a_0^2\ , \tag{37}$$

which is derived in Appendix A based on semiclassical arguments, and where the energies should be given in eV. For $n_e=10^{18}$ cm^{-3} and $k_BT=0.5$ eV, $\sigma_{\rm sc}\sim 3a_0^2$.

The quantum-mechanical differential cross section $\sigma(\theta,\phi)$ and the transition rate W are related by[23]

$$\sigma(\theta,\phi)=W/\Phi\ , \tag{38}$$

where Φ is the flux of incoming particles. For electrons with momentum $\hbar\mathbf{k}$,

$$\Phi_e=v_e/\Omega=\hbar k/\Omega m_e\ , \tag{39}$$

where Ω is the volume of the system. For a plasma in thermal equilibrium, the transition rate $W(vq/k)$ for an

electron with momentum $\hbar\mathbf{k}$ being captured by a fixed proton, into the state ν with emission of a plasmon of momentum $\hbar\mathbf{q}$, is given by[24]

$$W(\nu q/k)=(2\pi/\hbar)|(\nu q|T|k)|^2 f_k g_q \rho_q(E_q) , \tag{40}$$

with

$$\begin{aligned} f_k &= n_e(2\pi\hbar^2/m_e k_B T)^{3/2}\exp(-\hbar^2k^2/2mk_BT) , \\ g_q &= 1/[\exp(\hbar\omega_q/k_BT)-1] , \\ \rho_q(E_q) &= [\Omega/(2\pi)^3]q^2[d(\hbar\omega_q)/d_q]^{-1} \\ &= (\Omega/8\pi^3)(q/3\hbar\omega_p\lambda_D^2) , \end{aligned} \tag{41}$$

and with $(\nu q|T|k)$ the T matrix for the recombination transition. In (41), f_k is the electron distribution function nearly Maxwellian for the values of density and temperatures we are considering here, g_q is the plasmon (Bose-Einstein) distribution, much larger than unity in this case,[24] and $\rho_q(E_q)$ is the final-state density of plasmons. In leading order, the T matrix $(\nu q|T|k)$ reduces to the Hamiltonian matrix element $(\nu q|V(\mathrm{pl}\,a\leftarrow e)|k)$ given by (27), which can be rewritten as

$$(\nu q|V(\mathrm{pl}\,a\leftarrow e)|k) = \left[\frac{2\pi e^2\omega_q}{\Omega\hbar q^2}\right]^{1/2}\left[S_{qk\nu}-\sum_{k'}S_{qk\nu}\Delta_{\mathbf{k}',\mathbf{k}}\right] , \tag{42}$$

where

$$S_{qk\nu}=\Omega^{-1/2}\int d^3x\,\phi_\nu^*(\mathbf{x})e^{i(\mathbf{k}-\mathbf{q})\cdot\mathbf{x}}s_q(\mathbf{x}) , \tag{43}$$

with

$$s_q(\mathbf{x})=\sum_{K\,(>q_c)}\left[\frac{4\pi e^2}{\Omega K^2}\right]\left[\omega_q^{-1}-\left[\omega_q-\frac{\hbar\mathbf{q}\cdot\mathbf{K}}{m_e}\right]^{-1}\right]e^{i\mathbf{K}\cdot\mathbf{x}} . \tag{44}$$

In (44) we have neglected the term $\hbar\mathbf{q}\cdot\mathbf{k}/m_e$ compared with ω_q (BG approximation). For $k_BT\sim0.5$ eV and $n_e\sim10^{18}$ cm^{-3}, the error is less than 5% in the worst case that occurs when $q\sim q_c\sim\lambda_D^{-1}$, and $\mathbf{k}$ and $\mathbf{q}$ are parallel. The first term in (42) represents the Born approximation for the T-matrix elements, and the second term arises as a consequence of orthogonalizing the k dependence of the matrix elements to the bound-electron subspace. Since in the representation developed in Sec. III the effective interaction between the particles is so greatly reduced, we expect the Born approximation, to which we shall restrict the present calculations, to be a good first approximation.

To evaluate $s_q(\mathbf{x})$ we note that for $K\le q_c$ the term inside the square bracket in (44) vanishes in the BG approximation, and so the constraint $K>q_c$ in the summation can be dropped. Thus, in the continuum limit $[\sum_K\rightarrow(\Omega/8\pi^3)\int d^3K]$,

$$s_q(\mathbf{x})=-\frac{e^2}{2\pi^2\omega_q}\mathrm{P}\int d^3K\frac{e^{i\mathbf{K}\cdot\mathbf{x}}}{K^2}\frac{\epsilon_q\cdot\mathbf{K}}{(m_e/\hbar q)\omega_q-\epsilon_q\cdot\mathbf{K}} , \tag{45}$$

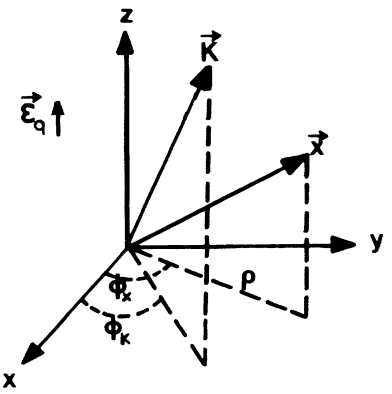

FIG. 8. Spatial arrangement of vectors $\mathbf{K}$, $\mathbf{q}$, and $\mathbf{x}$ for the evaluation of the integral $s_q(\mathbf{x})$.

where ϵ_q is a unit vector in the plasmon direction, and P in front of the integral means we take the principal value.[25] The singularity at $\epsilon_q\cdot\mathbf{K}=(m_e/\hbar q)\omega_q$ is isolated to one dimension by use of cylindrical coordinates with z axis parallel to ϵ_q as shown in Fig. 8. Complex integration allows us, in Appendix B, to reduce (45) to

$$s_q(\mathbf{x})=\pm\frac{m_e e^2}{\hbar q}i\left[K_0\left[\frac{m_e\rho\omega_q}{\hbar q}\right]e^{\pm i(m_e/\hbar q)\omega_q|z|} - I_1(\rho,|z|)\mp iI_2(\rho,|z|)\right] , \tag{46}$$

where the upper (lower) sign is valid for $z\ge0$ ($z<0$). In (46), $K_0(x)$ is the modified Bessel function of zeroth order, and I_1 and I_2 are given by

$$\begin{aligned} I_1(\rho,|z|) &= \int_0^\infty du\frac{uJ_0(m_e\rho\omega_q u/\hbar q)}{u^2+1}e^{-(m_e/\hbar q)\omega_q|z|u} , \\ I_2(\rho,|z|) &= \int_0^\infty du\frac{u^2J_0(m_e\rho\omega_q u/\hbar q)}{u^2+1}e^{-(m_e/\hbar q)\omega_q|z|u} . \end{aligned} \tag{47}$$

These integrals cannot be solved in closed form for arbitrary values of ρ and z. However, when

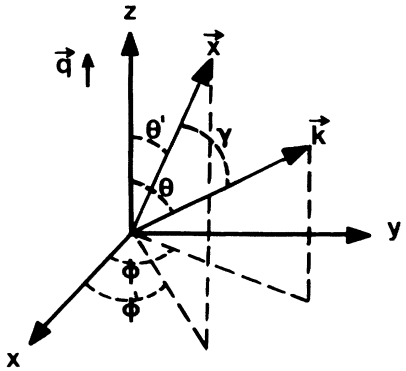

FIG. 9. Spatial arrangement of vectors $\mathbf{q}$, $\mathbf{x}$, and $\mathbf{k}$ for the evaluation of $S_{qk\nu}$.

$(m_e/\hbar q)\omega_q|z| \gg 1$, the main contribution to the integrals arise from the range $u \ll 1$, making it possible to expand the factor $(u^2+1)^{-1}$ in terms of a series of powers of u and to solve the integrals analytically. In the course of solving S_{qkv}, we shall find that $(m_e/\hbar q)\omega_q|z|$ is indeed much larger than one, but for the moment we choose to keep I_1 and I_2 in integral form.

S_{qkv} is evaluated in spherical coordinates with $\mathbf{q}$ along the z axis as shown in Fig. 9. Then $\mathbf{q}\cdot\mathbf{x}=qr\cos\theta'$ and $\mathbf{k}\cdot\mathbf{x}=kr\cos\gamma=kr[\cos\theta\cos\theta'+\sin\theta\sin\theta'\cos(\phi-\phi')]$.[26] The wave function $\phi_v(\mathbf{x})$ with $v=(nlm)$ is[27]

$$\phi_v(\mathbf{x})=C_l^m\frac{u_{n,l}(r)}{r}P_l^m(\cos\theta')e^{-im\phi'}, \qquad C_l^m\equiv\left[\frac{2l+1}{4\pi}\frac{(l-m)!}{(l+m)!}\right]^{1/2}, \tag{48}$$

where the functions $u_{n,l}(r)$ are taken to be the solutions of the radial Schrödinger equation for the Debye-Hückel potential. The function $s_q(\mathbf{x})$ is a function of ρ and z; therefore, with $\rho=r\sin\theta'$ and $z=r\cos\theta'$, we have $s_q(\mathbf{x})=s_q(r,\theta')$. Thus

$$S_{qkv}=C_l^m\Omega^{-1/2}\int_0^\infty dr\, ru_{n,l}(r)\int_0^\pi d(-\cos\theta')e^{i(k\cos\theta-q)r\cos\theta'}s_q(r,\theta')P_l^m(\cos\theta')\int_0^\infty d\phi' e^{-i[m\phi'-kr\sin\theta\sin\theta'\cos(\phi-\phi')]}. \tag{49}$$

Doing the change of variables $x=r/a_0$ (a_0 the Bohr radius) and $y=\cos\theta'$, defining $\delta_1\equiv ka_0\sin\theta$, $\delta_2\equiv(k\cos\theta-q)a_0$, and using the integral representation of the Bessel function of order m,[26] we obtain

$$S_{qkv}=\frac{2\pi a_0^{3/2}}{\Omega^{1/2}}i^m e^{-im\phi}C_l^m\int_0^\infty dx\, xu_{n,l}(x)\int_{-1}^1 dy\, s_q(x,y)P_l^m(y)J_m(\delta_1 x\sqrt{1-y^2})e^{i\delta_2 xy}. \tag{50}$$

We note that the argument of the Bessel function is an even function of y, and that the associated Legendre polynomials $P_l^m(y)$ satisfy the relation[26] $P_l^m(-y)=(-1)^{l+m}P_l^m(y)$. The other two terms in (50) can also be written as sums of odd and/or even functions of y. With all this we can change the range of the y integration to [0,1]. Replacing (46) and (47) into (50) and changing the range of the y integration yields

$$S_{qkv}=\frac{4\pi m_e e^2 a_0^{3/2}}{\hbar q\Omega^{1/2}}i^m e^{-im\phi}\left[\frac{2l+1}{4\pi}\frac{(l-m)!}{(l+m)!}\right]^{1/2}\times\begin{cases}Z_1^{(e)}+Z_2^{(e)}+Z_3^{(e)}, & m+l \text{ even},\\ i(Z_1^{(o)}+Z_2^{(o)}+Z_3^{(o)}), & m+l \text{ odd},\end{cases} \tag{51}$$

with

$$Z_1^{(e)}=\int_0^\infty dx\, xu_{n,l}(x)\int_0^1 dy P_l^m(y)J_m(\delta_1 x(1-y^2)^{1/2})K_0(\Delta_q x(1-y^2)^{1/2})\times\begin{Bmatrix}-\sin\Delta_q xy\\ \cos\Delta_q xy\end{Bmatrix}, \tag{52}$$

$$Z_2^{(e)}=\int_0^\infty dx\, xu_{n,l}(x)\int_0^1 dy P_l^m(y)J_m(\delta_1 x(1-y^2)^{1/2})\times\begin{Bmatrix}\sin\delta_2 xy\\ -\cos\delta_2 xy\end{Bmatrix}\int_0^\infty du\frac{uJ_0(\Delta_q x(1-y^2)^{1/2}u)}{u^2+1}e^{-\Delta_q xyu}, \tag{53}$$

$$Z_3^{(e)}=\int_0^\infty dx\, xu_{n,l}(x)\int_0^1 dy P_l^m(y)J_m(\delta_1 x(1-y^2)^{1/2})\times\begin{Bmatrix}\cos\delta_2 xy\\ \sin\delta_2 xy\end{Bmatrix}\int_0^\infty du\frac{u^2J_0(\Delta_q x(1-y^2)^{1/2}u)}{u^2+1}e^{-\Delta_q xyu}, \tag{54}$$

where the density-independent quantity $\Delta_q\equiv(ma_0\omega_q/\hbar q)\geq 0.5$ for $k_BT\gtrsim 0.5$ eV. For highly excited states, the function $u_{n,l}(x)$ will have a large amplitude at large values of x. For example, for $\lambda_D\sim 100a_0$ we see from Fig. 10 that the amplitude of $u_{80}(x)$ is large for values of $x\gg 1$. The same is true for u_{81}. Therefore, as already mentioned before, the main contribution to the last integrals in $Z_2^{(e)}$ and $Z_3^{(e)}$ will come from a region $u\ll 1$. Doing the expansion[26]

$$(u^2+1)^{-1}=\sum_{s=0}^\infty(-1)^s u^{2s},$$

we have[26]

$$\int_0^\infty du\frac{uJ_0(\Delta_q x(1-y^2)^{1/2}u)}{u^2+1}e^{-\Delta_q xyu}=\sum_{s=0}^\infty(-1)^s\frac{(2s+1)!}{(\Delta_q x)^{2s+2}}P_{2s+1}(y), \tag{55}$$

$$\int_0^\infty du\frac{u^2J_0(\Delta_q x(1-y^2)^{1/2}u)}{u^2+1}e^{-\Delta_q xyu}=\sum_{s=0}^\infty(-1)^s\frac{(2s+2)!}{(\Delta_q x)^{2s+3}}P_{2s+2}(y). \tag{56}$$

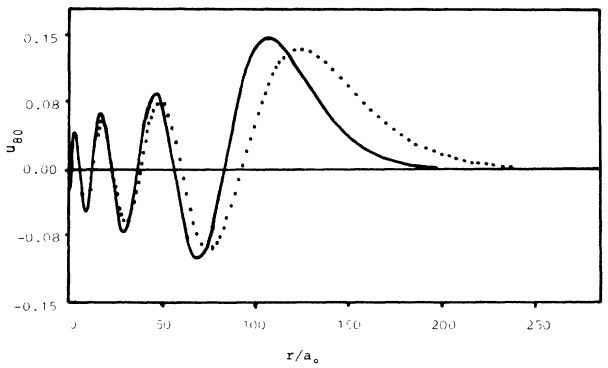

FIG. 10. Eigenfunction $u_{80}(r)=rR_{80}(r)$ for $\lambda_D=\infty$ (solid line) and $\lambda_D=100a_0$ (dotted line).

Because $\Delta_q x \gg 1$ and $|P_l(y)| \leq 1$ for the range $0 \leq y \leq 1$, then we keep only the first term in the series (55) and (56), an approximation which will be verified later by explicit calculations. Thus the integrals $Z_2^{(e_o)}$ and $Z_3^{(e_o)}$ can be rewritten in the approximated form

$$Z_2^{(e_o)} \cong \Delta_q^{-1} \int_0^\infty dx \frac{u_{n,l}(x)}{(\Delta_q x)} \int_0^1 dy P_l^m(y) J_m(\delta_1 x (1-y^2)^{1/2}) y \times \begin{Bmatrix} \sin\delta_2 xy \\ -\cos\delta_2 xy \end{Bmatrix}, \quad (57)$$

$$Z_3^{(e_o)} \cong \Delta_q^{-1} \int_0^\infty dx \frac{u_{n,l}(x)}{(\Delta_q x)^2} \times \int_0^1 dy P_l^m(y) J_m(\delta_1 x (1-y^2)^{1/2})(3y^2-1) \times \begin{Bmatrix} \cos\delta_2 xy \\ \sin\delta_2 xy \end{Bmatrix}. \quad (58)$$

Therefore, with (51) and (52) and (57) and (58), S_{qkv} is given in terms of three two-dimensional integrals, which can be solved numerically without many complications.

The differential cross section, in Born approximation, for plasmonic recombination is with (40), (41), and (51)

$$\sigma_{nlm}^{(\mathrm{Born})}(\theta,\phi) = \frac{2}{3} \frac{\lambda_D/a_0}{(ka_0)(q\lambda_D)^3} \frac{(2l+1)(l-m)!}{(l+m)!} \times |Z_1+Z_2+Z_3|^2 f_k g_l a_0^2 . \quad (59)$$

Taking $n_e = 10^{18}$ cm^{-3}, $k_B T = 0.5$ eV, and $(q\lambda_D)^2 = 0.1$, we have for all the levels with $m = 0$

$$\sigma_{nlo}^{(\mathrm{Born})}(\theta,\phi) = \frac{24.1}{ka_0}(2l+1)|Z_1+Z_2+Z_3|^2 \times e^{-\hbar^2 k^2/2m_e k_B T} a_0^2 , \quad (60)$$

with k fixed by $\hbar\omega_l$ and ε_{nl} through the conservation of the energy. The radial wave functions $u_{n,l}(x)$ appearing in the integrals Z_j $(j=1,2,3)$, and the corresponding eigenenergies $\varepsilon_{n,l}$ were obtained numerically[28] by integration of the Schrödinger equation for the screened Coulomb (Debye-Hückel) potential. The analytic solutions for the (unscreened) Coulomb potential were used to check the program. The results agree up to four decimal places. The eigenenergies were also compared with the results of Rogers, Graboske, and Harwood and Roussel and O'Connell[2] which represent the most complete references in this problem. Our results for $\lambda_D = 100a_0$ agree well with those of Rogers, Graboske, and Harwood, except for the bound states $9i$ and $9k$, with energies 3.3×10^{-4} and 2.0×10^{-5} Ry, respectively, not explicitly reported in their Table II, but implicitly included through their Table III.[29] This situation had been previously reported by Roussel and O'Connell, who obtained for these states the same energies. The two-dimensional integrals Z_j were solved by semiopen trapezoidal routines[30] (for the x integrals) and by N points Gauss-Legendre routines[30] (for the y integrals) where N was varied from 10 to 64 with the results differing by less than 1%. The results for the differential cross sections are

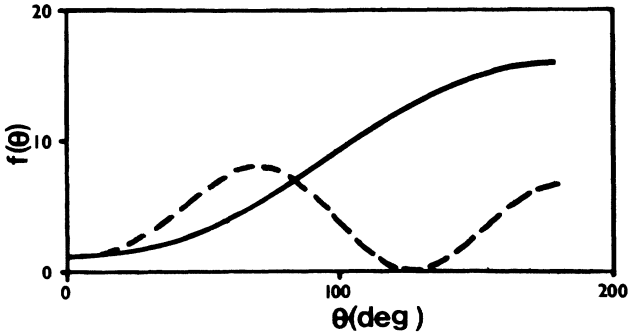

FIG. 11. Functions $f_{80}(\theta)$ (solid line) and $f_{81}(\theta)$ (dashed line).

$$\begin{aligned} \sigma_{800}^{(\mathrm{Born})}(\theta) &= 5.34 f_{80}(\theta) a_0^2 , \\ \sigma_{900}^{(\mathrm{Born})}(\theta) &= 4.26 f_{90}(\theta) a_0^2 , \\ \sigma_{810}^{(\mathrm{Born})}(\theta) &= 0.67 f_{81}(\theta) a_0^2 , \\ \sigma_{910}^{(\mathrm{Born})}(\theta) &= 1.69 f_{91}(\theta) a_0^2 , \end{aligned} \quad (61)$$

with the functions $f_{nl}(\theta)$ displayed in Figs. 11 and 12.

In Born approximation it is possible to evaluate the matrix elements (42) without neglecting the term $\hbar\mathbf{q}\cdot\mathbf{k}/m_e$ compared with ω_l as was done in (44).[31] The difference between the two results for the case of transitions into the state $8s$ is 2.3%, which is lower than our estimated maximum error of 5%. The contributions from the integral Z_3 were found to be less than 1% of those from Z_1+Z_2 for all the cases, something which might be understood from the fact that there is an extra factor $(\Delta_q x)^{-1}$ in the integrand of Z_3 as compared with Z_2, together with the fact that the important contribution to the x integral comes from the range $\Delta_q x \sim 10^2$. The integrals Z_2' and Z_3' arising from the second terms in the expansions (55) and (56) gave values that were four orders-of-magnitude smaller than Z_2 and Z_3. Again this is to be expected because the integrands of Z_2' and Z_3' contain extra factors $(\Delta_q x)^{-2}$ as compared with those of Z_2 and Z_3, respectively. Therefore, the approximations (57) and (58) to Z_2 and Z_3 are totally justified.

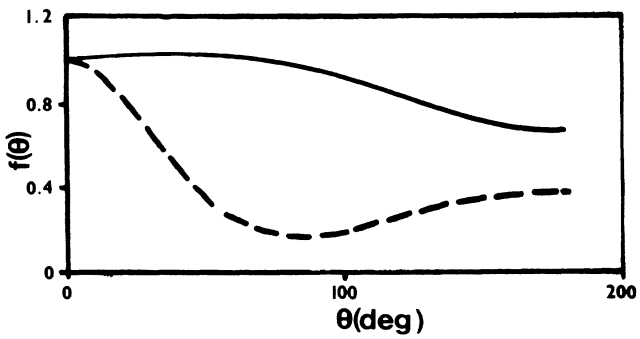

FIG. 12. Functions $f_{90}(\theta)$ (solid line) and $f_{91}(\theta)$ (dashed line).

Comparing (61) with the semiclassical result, we see that there is a fair agreement between the semiclassical estimate and the formal quantum-mechanical calculations of plasmonic recombination cross sections, especially for small angles where $f_{nl}(\theta)\sim 1$. To get an idea of the importance of the collective mechanism, we would have to compare it with the usual radiative and three-body modes. For the highly excited and perturbed (screened) levels of hydrogen such calculations have not been done for the values of density and temperature assumed here. However, from Bethe and Salpeter[27] we can obtain a rough estimate for radiative recombination cross sections (in vacuum) into the levels $n=8,9$ of hydrogen. The cross sections for the radiative mode are found to be at least five orders-of-magnitude smaller than those of the plasmonic mode. The effect of the smallness of the plasmon phase space (as compared with the full photon phase space) due to the constraint $q<q_c$ will tend to be canceled by the effect of screening on the radiative cross sections,[3,14] but a final conclusion must await more detailed calculations. On the other hand, it is known that the excitation of plasmons makes a contribution to the stopping power of the plasma that is comparable to that of the short-range (two-body) charged-particle interactions.[6] This suggests that three-body recombination and the plasmonic mode may be of comparable importance. Recent calculations[21] show this to be the case at metallic densities. In connection with this we should remark that since screening leads to a finite and small number of bound states, and since plasmonic recombination to low-lying levels of hydrogen are not energetically allowed as real processes, the region of the energy-level spectrum in which the plasmonic mode might be important is very narrow ($8\leq n\leq 9$, for $n_e=10^{18}$ cm^{-3} and $k_BT=0.5$ eV).[14] In this region our use of static rather than dynamic screening should be a good first approximation.

V. CONCLUSION

The Bohm-Pines Fock-Tani representation for a fixed proton immersed in a finite-temperature electron gas was obtained. The major feature of the representation can be summarized as follows.

(i) The particles in the system interact individually through short-range screened Coulomb potentials. Screening, which tends to reduce the cross sections[3] for hydrogenic transitions of the highest-bound states with respect to their vacuum values, is contained in all the matrix elements for the different channels in the Hamiltonian.

(ii) Long-range interactions are accounted for by the emission or absorption of plasmons. This leads to dynamical effects caused by the medium as a whole. In some sense the medium behaves as if it were a third particle that (by participating dynamically) allows several novel processes to occur.

(iii) Different scattering and reactions channels are easily identified by looking for the terms in the Hamiltonian involving the right combination of creation and annihilation operators for the reacting particles.

The first two features characterize the BP collective representation[5] of the system, and the last one appears as a result of describing atoms by elementary operators in Fock-Tani representation.[16,17] An important consequence of the above is that we explicitly exhibit a series of collective mechanisms for atomic processes in plasmas such as bound-bound and free-free transitions of electrons in the field of the proton with emission or absorption of plasmons. Another consequence of the representation, which was already mentioned in Ref. 4, is that the negative shifts Δ of the energy due to absorption and emission of virtual plasmons by the particles of the system give rise to an effective potential for the hydrogen atom in the electron gas, which is very similar to the Ecker-Weizel potential used to interpret the plasma shifts of the discrete and continuous spectra of hydrogen.[32]

As an application of the representation, we evaluated cross sections (in Born approximation) for plasmon-mediated recombination into the highly excited and perturbed levels of hydrogen for plasma conditions such as those occurring in stellar atmospheres. The plasmonic cross sections appear to be much larger than those for the radiative mechanism and might be even comparable or larger than those for the three-body mode as Rasolt and Perrot[21] recently found for Al at metallic densities and temperatures of the order of 100 eV. These results could have strong implications for the basic theory of radiative equilibrium of partially ionized plasmas and also in predicting and diagnosing the state of high-density laboratory systems.

In a future work, we hope to include orthogonalization corrections and higher-order approximations for the matrix elements of plasmon-mediated recombination of hydrogen for temperatures and densities ranging from those of stellar atmospheres ($n_e\sim 10^{15}$–10^{18} cm^{-3}, $k_BT\sim 0.5$–5 eV) up to those relevant to recombination x-ray laser experiments ($n_e\sim 10^{21}$ cm^{-3}, $k_BT\sim 100$ eV) and laser inertial confinement fusion (ICF) ($n_e\sim 10^{23}$–10^{26} cm^{-3}, k_BT is several keV).

ACKNOWLEDGMENTS

The initial phases of this research at the University of Oregon were supported by the Office of Naval Research. The work was completed at the Institute for Theoretical Physics (ITP), University of California, Santa Barbara, where it was supported by the National Science Foundation under Grant No. PHY82-17853, supplemented by funds from the National Aeronautics and Space Administration. One of us (F.A.G.) is indebted to the Fundación Andes for the special grant that allowed him to participate in the program "Atoms and ions in strongly coupled plasmas" at the ITP, and to the Dirección de Investigación and the Vicerrectoría Académica de la Universidad de Concepción for their additional support.

APPENDIX A: ESTIMATE FOR σ_{sc}

The mean free path for plasmon emission by an electron with velocity v and energy E is[33]

$$\lambda=\frac{\hbar\omega_p E}{2\pi n_e e^4\ln(q_c v/\omega_p)}\ . \tag{A1}$$

Taking $q_c\sim(\sqrt{4\pi}\lambda_D)^{-1}$, so that the condition $q_c\lambda_D<1$ is

satisfied, yields for the critical velocity

$$v_c \sim \omega_{q_c}/q_c \sim (4\pi k_B T/m_e)^{1/2} , \tag{A2}$$

and for the critical kinetic energy

$$E_c = \tfrac{1}{2} m v_c^2 \sim 2\pi k_B T . \tag{A3}$$

From the semiclassical picture of Fig. 13, for the recombination process the probability of plasmon emission by the electron in the field of the proton is

$$P \sim \pi a/\lambda , \tag{A4}$$

with a the impact parameter of the incoming electron, which must be small enough for a low- (zero) velocity electron to be accelerated to E_c at perihelion:

$$E_{\text{tot}} = 0 = E_c - e^2/a , \tag{A5}$$

so that

$$a = e^2/E_c = \frac{\mathcal{R}}{\pi k_B T} a_0 , \tag{A6}$$

with E_{tot} the total energy, $\mathcal{R}$ the Rydberg constant, and a_0 the Bohr radius. For $k_B T \gtrsim 0.5$ eV and $n_e \gtrsim 10^{18}$ cm^{-3}, then $a/\lambda_D \lesssim 0.086 \ll 1$, so that the use of the unscreened Coulomb potential in (A5) is justified for the present purposes. The semiclassical cross section σ_{sc} is

$$\sigma_{\text{sc}} \simeq \pi a^2 P f_{\text{low}} g_{\text{pl}} . \tag{A7}$$

Here f_{low} is the fraction of the total number of electrons with momentum less than $p_{\max}$, where $p_{\max} \sim (m_e \hbar\omega_p)^{1/2}$ is the maximum momentum allowed by conservation of energy for the plasmon emission, and g_{pl} is the plasmonic distribution function which is introduced to take into account the plasmon degeneracy. They are given by

$$f_{\text{low}} \cong \frac{\int_{p<p_{\max}} e^{-p^2/2mk_B T} d^3p}{\int_{\text{all } p} e^{-p^2/2mk_B T} d^3p} \sim \frac{1}{3}\left[\frac{2}{\pi}\right]^{1/2}\left[\frac{\hbar\omega_p}{k_B T}\right]^{3/2} , \tag{A8}$$

$$g_{\text{pl}} \approx (e^{\hbar\omega_q/k_B T} - 1)^{-1} \approx \frac{k_B T}{\hbar\omega_p}, \quad \text{for } k_B T \gg \hbar\omega_q . \tag{A9}$$

Replacing (A1)–(A4) (with $v = v_c$ and $E = E_c$) and (A6) into (A7), and since $\ln(q_c v_c/\omega_p) \sim 1$, we obtain, with (A8) and (A9), expression (37).

APPENDIX B: THE INTEGRAL $s_l(\mathbf{x})$

With (45) and Fig. 8, we have $\epsilon_q \cdot \mathbf{K} = K_z$, $\mathbf{K}\cdot\mathbf{x} = K_\perp \cos(\phi_K - \phi_x) + K_z Z$, and[26]

$$s_q(\mathbf{x}) = \frac{-e^2}{\pi\omega_q} \mathrm{P}\int_{-\infty}^{\infty} dK_z \frac{K_z e^{iK_z Z}}{(m_e/\hbar q)\omega_q - K_z} \times \int_0^{\infty} dK_\perp \frac{K_\perp J_0(\rho K_\perp)}{K_\perp^2 + K_Z^2} , \tag{B1}$$

where $J_0(u)$ is the zeroth-order Bessel function. Defining $t = \rho K_\perp$, $p = \rho K_z$, $a = (m/\hbar q)\rho\omega_q$, and $b = z/\rho$, and interchanging the order of the integrals in (B1) yields

$$s_q(\mathbf{x}) = \frac{e^2}{\pi\rho\omega_q} \int_0^{\infty} dt\, t J_0(t) \left[\mathrm{P}\int_{-\infty}^{\infty} dp \frac{p e^{ibp}}{p-a} \frac{1}{p^2+t^2}\right] . \tag{B2}$$

The integral inside the large parentheses is solved using complex integration. In the complex ω plane, we close the contour in the upper half plane for $b > 0$, and in the lower half plane for $b < 0$, as shown in Fig. 14. The poles are at $\omega = \pm it$ and $\omega = a$. The contribution from the path C_R ($C_{R'}$) to the integral from $b > 0$ ($b < 0$) vanishes as $|\omega|^{-1}\exp(-|b|\mathrm{Im}\omega)$ when the limit $|\omega| \to \infty$ is taken.

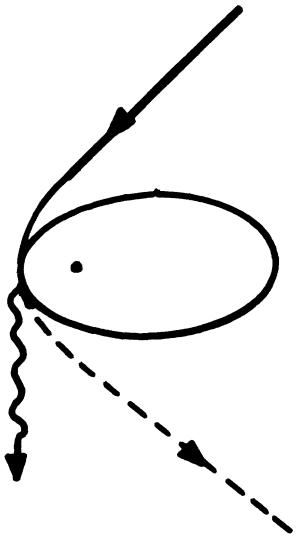

FIG. 13. Semiclassical picture for plasmonic recombination.

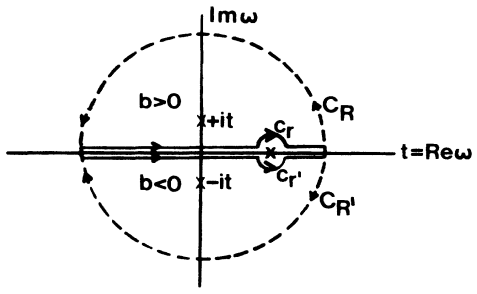

FIG. 14. Integration contours for the evaluation of the principal-value integral in (B2).

Therefore, Cauchy's theorem and the calculus of residues give[34]

$$s_q(\mathbf{x})=\pm\frac{e^2}{\rho\omega_q}i\int_0^\infty dt\frac{tJ_0(t)}{t^2+a^2}(ae^{\pm i|b|a}-ae^{-|b|t}\mp ite^{-|b|t}) , \tag{B3}$$

where the upper (lower) sign is valid for $b\geq 0$ ($b<0$). Setting $t=au$, using the integral representation of the modified Bessel function of zeroth-order $K_0(xy)$,[26]

$$K_0(xy)=\int_0^\infty du\frac{J_0(xu)}{u^2+y^2} , \tag{B4}$$

and replacing explicitly the expressions for a and b, we obtain after some algebra relation (46). It is possible to obtain the same result without changing the order of the integrals in (B1), although the calculations are more laborious. To show it we use (B4) to rewrite (B1) as

$$s_q(\mathbf{x})=\frac{e^2}{\pi\rho\omega_q}\times\begin{cases}I_A^>+I_B^> & \text{if } b>0 ,\\ I_A^<+I_B^< & \text{if } b<0 ,\end{cases} \tag{B5}$$

with

$$I_A^{(\gtrless)}=\int_0^\infty dt\frac{te^{-ibt}}{t+a}K_0(t) \quad \text{if } b\gtrless 0 , \tag{B6}$$

$$I_B^{(\gtrless)}=\mathrm{P}\int_0^\infty dt\frac{te^{ibt}}{t-a}K_0(t) \quad \text{if } b\gtrless 0 , \tag{B7}$$

and with a and b as in (B2). Using the complex-ω plane (see Fig. 15), Cauchy's theorem, and the calculus of residues, one has[34]

$$I_A^{(\gtrless)}=-\int_0^\infty dt\frac{te^{-|b|t}}{a\mp it}K_0(\mp it) \quad \text{if } b\gtrless 0 , \tag{B8}$$

$$I_B^{(\gtrless)}=\pm i\pi aK_0(a)e^{\pm i|b|a}+\int_0^\infty dt\frac{te^{-|b|t}}{a\mp it}K_0(\pm it) \quad \text{if } b\gtrless 0 . \tag{B9}$$

The contributions of $C_{R_A}^{(+)}$, $C_{R_A}^{(-)}$, $C_{R_B}^{(+)}$, and $C_{R_B}^{(-)}$ to $I_A^>$, $I_A^<$, $I_B^>$, and $I_B^<$, respectively, will be shown to vanish.

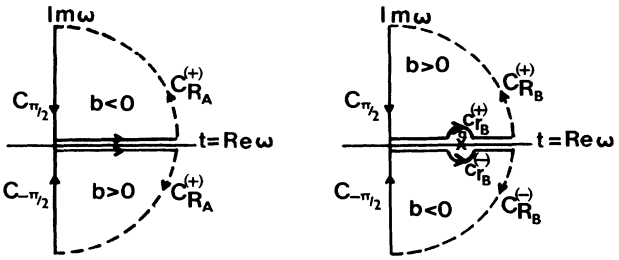

FIG. 15. Integration contours for the evaluation of $I_A^{(\gtrless)}$ and $I_B^{(\gtrless)}$ in Appendix B.

The analytic continuation of the modified Bessel functions $K_\nu(z)$ and $I_\nu(z)$,[30]

$$K_\nu(ze^{im\pi})=e^{-im\nu\pi}K_\nu(z)-i\pi\sin(m\nu\pi)\csc(\nu\pi)I_\nu(z), \tag{B10}$$

$$I_\nu(ze^{im\pi})=e^{im\nu\pi}I_\nu(z) , \tag{B11}$$

with m an integer, and the relation $I_0(z)=J_0(iz)$ with z a complex number, allows us to write

$$I_A^>+I_B^>=i\pi ae^{i|b|a}K_0(a)-i\pi\int_0^\infty dt\frac{tJ_0(t)}{t^2+a^2}(a+it)e^{-|b|t} , \tag{B12}$$

$$I_A^<+I_B^<=-i\pi ae^{-i|b|a}K_0(a)+i\pi\int_0^\infty dt\frac{tJ_0(t)}{t^2+a^2}(a-it)e^{-|b|t} . \tag{B13}$$

Therefore, (B5), (B12), and (B13) together with (B4) give (B3), which is the result we were trying to obtain. It remains to show that the contributions from the large semicircular paths in Fig. 15 vanish. For large $|\omega|$, $K_0(\omega)$ behaves as[30]

$$K_0(\omega)\sim(\pi/2\omega)^{1/2}e^{-\omega}(1-1/\omega+\cdots) ; \tag{B14}$$

therefore, for $b>0$, and with $R_A=|\omega|$, we have with (B14)

$$\lim_{R_A\to\infty}\int_{C_{R_A}^{(-)}}d\omega\frac{\omega e^{-ib\omega}}{\omega+a}K_0(\omega) \leq\lim_{R_A\to\infty}\frac{\pi R_A}{2}\max\left|\frac{\omega e^{-ib\omega}K_0(\omega)}{\omega-a}\right|=0 . \tag{B15}$$

Similar arguments give the same results for $C_{R_A}^{(+)}$, $C_{R_B}^{(-)}$, and $C_{R_B}^{(+)}$.

[1]S. Ichimaru, *Basic Principles of Plasma Physics: A Statistical Approach* (Benjamin/Cummings, Reading, MA, 1973).
[2]F. J. Rogers, H. C. Graboske, and D. J. Harwood, Phys. Rev. A **1**, 1577 (1970); K. M. Roussel and R. F. O'Connell, Phys. Rev. A **9**, 52 (1974).
[3]J. C. Weisheit, in *Plasmas*, Vol. 2 of *Applied Atomic Collision Physics*, edited by H. S. W. Massey, E. W. McDaniel, and B. Bederson (Academic, New York, 1984), p. 441ff; J. C. Weisheit, in *Advances in Atomic and Molecular Physics*, edited by D. Bates and B. Bederson (Academic, New York, 1988), Vol. 25, p. 101ff.
[4]M. D. Girardeau and F. A. Gutierrez, Phys. Rev. A **38**, 1624 (1988).
[5]D. Bohm and D. Pines, Phys. Rev. **98**, 609 (1953).
[6]D. Pines and D. Bohm, Phys. Rev. **85**, 338 (1952).

[7]D. Pines and J. R. Schrieffer, Phys. Rev. **125**, 804 (1962).

[8]D. Bohm and E. P. Gross, Phys. Rev. **75**, 1851 (1949).

[9]Assuming an isotropic distribution of velocities, Bohm and Gross (Ref. 8) obtained the more general expression $\omega_q^2=\omega_p^2+\langle v^2\rangle q^2$ for small q, which reduces to (3) for a Maxwellian distribution.

[10]The unphysical oscillations in the tail of the short-range potential $V_{e\text{-}e}$ are a consequence of the sharp cutoff in momentum space introduced in the theory to separate the long-range part of the interaction from the short-range part. Such a cutoff does not exist for the finite-temperature electron gas; instead there is a smooth transition near $q_c\sim\lambda_D^{-1}$, where the system goes from weak to strong damping. Fortunately, these oscillations which are present beyond a distance $2\lambda_D$ (see Ref. 5, p. 613) are very small, comparable to the terms neglected in getting the Hamiltonian (1); so they can be neglected.

[11]See D. Bohm and D. Pines, Ref. 5, p. 614, Eq. (25).

[12]L. D. Landau, J. Phys. Moscow **10**, 25 (1946).

[13]See D. Bohm and D. Pines, Ref. 5, p. 617, Eq. (51).

[14]F. A. Gutierrez, Ph.D. dissertation, University of Oregon, 1988 (unpublished).

[15]The analysis about the oscillations in $V_{e\text{-}e}$ given in Ref. 10 also apply to this electron-proton interaction term which in coordinate space can be represented to a good approximation by the potential $-\sum_i (e^2/r_i)e^{-q_c r_i}$, where r_i is the distance between the proton and the ith electron.

[16]M. D. Girardeau, J. Math. Phys. **16**, 1901 (1975).

[17]M. D. Girardeau, Phys. Rev. A **26**, 217 (1982), and references therein.

[18]We use the same notation and the same kind of diagrams as in Ref. 16.

[19]A. L. Fetter and J. D. Walecka, *Quantum Theory of Many-Particle Systems* (McGraw-Hill, New York, 1971).

[20]Orthogonalized plane waves (OPW) have been used in calculations of photionization cross sections of molecules. See M. Mishra and Y. Öhrn, Int. J. Quantum Chem. Symp. **14**, 334 (1980), and references therein.

[21]M. Rasolt and F. Perrot, Phys. Rev. Lett. **62**, 2273 (1989).

[22]We use the eigenvalues for the screened Coulomb Debye-Hückel potential. See, for example, F. J. Rogers, H. C. Graboske, and D. J. Harwood, in Ref. 2, p. 1582, Table II.

[23]J. C. Joachain, *Quantum Collision Theory* (North-Holland, Amsterdam, 1983).

[24]See M. D. Girardeau and F. A. Gutierrez, Ref. 4, p. 1627. The replacement of the statistical factor $1+\langle\hat{N}_q\rangle=1+\langle\hat{C}_q^{\dagger}\hat{C}_q\rangle$ by unity in their Eq. (21) is incorrect because for the temperatures and densities under consideration $\langle\hat{N}_q\rangle\gg1$. Therefore, $1+\langle\hat{N}_q\rangle\approx\langle\hat{N}_q\rangle\equiv g_q$ is the right approximation.

[25]The other two obvious choices [adding the imaginary infinitesimal $\pm i\eta$ to the denominator in the integrand of (45)] were disregarded because they would make the BP canonical transformation (see Ref. 13) not unitary.

[26]S. Gradshteyn and I. M. Ryzhik, *Tables of Integrals, Series, and Products* (Academic, New York, 1980).

[27]H. A. Bethe and E. E. Salpeter, *Quantum Mechanics of One- and Two-Electron Atoms* (Plenum, New York, 1977).

[28]We are indebted to Dr. Chris Nex for sending us his code to solve the Schrödinger equation.

[29]F. J. Rogers (private communication).

[30]M. Abramowitz and I. A. Stegun, *Handbook of Mathematical Functions* (Dover, New York, 1968).

[31]Although it is possible to evaluate $s_q(\mathbf{x})$ in (44) keeping the term $\hbar\mathbf{q}\cdot\mathbf{k}/m_e$ coming from (12), it has to be neglected to be consistent with the BG approximation. This approximation also helps to evaluate the orthogonalization terms in the matrix elements (42) (see Ref. 14).

[32]W. D. Kraeft, D. Kremp, W. Ebeling, and G. Röpke, *Quantum Statistics of Charged Particle Systems* (Plenum, New York, 1986), p. 137ff.

[33]D. Pines, Phys. Rev. **92**, 626 (1953), p. 634ff.

[34]E. Butkov, *Mathematical Physics* (Addison-Wesley, New York, 1975).